Gas-Phase Photolysis of Pyruvic Acid: The Effect of Pressure on Reaction Rates and Products

Allison E. Reed Harris,[†] Jean-Francois Doussin,[‡] Barry K. Carpenter,[§] and Veronica Vaida*[,†]

[†]Department of Chemistry and Biochemistry, CIRES, University of Colorado, Boulder, Colorado 80309, United States
[‡]LISA, UMR-CNRS 7583, Université Paris Est Creteil (UPEC), Université Paris Diderot (UPD), Institut Pierre Simon Laplace (IPSL), 94010 Creteil, France
[§]School of Chemistry, Cardiff University, Cardiff CF10 3AT, U.K.

* Supporting Information

ABSTRACT: In this work, we investigate the impact of pressure and oxygen on the kinetics of and products from the gas-phase photolysis of pyruvic acid. The results reveal a decrease in the photolysis quantum yield as pressure of air or nitrogen is increased, a trend not yet documented in the literature. A Stern Volmer analysis demonstrates this effect is due to deactivation of the singlet state of pyruvic acid when the photolysis is performed in nitrogen, and from quenching of both the singlet and triplet state in air. Consistent with previous studies, acetaldehyde and CO_2 are observed as the major products; however, other products, most notably acetic acid, are also identified in this work. The yield of acetic acid increases with increasing pressure of buffer gas, an effect that is amplified by the presence of oxygen. At least two mechanisms are necessary to explain the acetic acid, including one that requires reaction of photolysis intermediates with O_2. These findings extend the fundamental understanding of the gas-phase photochemistry of pyruvic acid, highlighting the importance of pressure on the photolysis quantum yields and products.

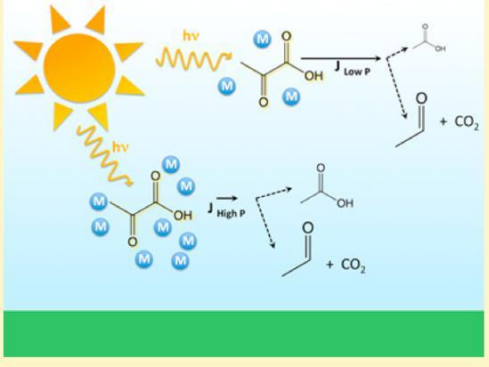

I. INTRODUCTION

Sunlight is the major source of energy for Earth's atmospheric chemistry.[1−4] Photochemical reactions determine the composition of the atmosphere through direct photolysis, and by the formation of reactive species, such as the hydroxyl radical, which trigger regionally defining chemical cycles.[5] For example, processing of volatile organic compounds (VOCs), which have an annual emission budget of 1300 Tg C/yr,[6,7] in the presence of $^{\bullet}OH$ is related to the formation of smog, haze, and secondary organic aerosol.[8−10] While many VOCs found in the troposphere are removed most efficiently through oxidation by the hydroxyl radical,[8,9] direct photolysis can become important if the molecule has absorption features in the actinic range and its reaction with $^{\bullet}OH$ is slow, as is the case for some carbonyl compounds.[11−14] Further, a few aldehydes and ketones have demonstrated a photolysis quantum yield that is dependent on pressure, and, by extension, altitude.[15−17] In these instances, it is of fundamental and practical importance to understand the photophysical and photochemical properties that are determining factors in the lifetime and atmospheric impact of the involved molecules, including their absorption cross sections, reaction pathways, and quantum yields.[8,18,19]

Pyruvic acid, formed in the oxidative processing of isoprene,[20−22] is one compound removed from the atmosphere primarily by direct photolysis, while reaction with $^{\bullet}OH$ and wet deposition act as secondary sinks.[12,18] It has been detected in the gas phase (10−100 ppt), in aerosol (up to 140 ng m^{-3}), and in snow and rainwater[21,23−35] and, therefore, is a molecule of interest to many aspects of atmospheric research.[18,36−50] Laboratory studies of pyruvic acid have investigated a variety of reactions, including gas- and condensed-phase photolysis,[12,51,52] radical oxidation,[53] thermal decomposition,[54] multiphoton pyrolysis,[55] and vibrational overtone induced decarboxylation.[56−58] Computational studies on pyruvic acid's electronic structure, conformational possibilities, and barriers to decarboxylation complement and confirm the available experimental results.[41,59−63] Laboratory studies of the photochemistry of pyruvic acid in both the gas and aqueous phase began in the 1960s; however, it is not completely clear how results from these early studies apply to chemistry in the troposphere.[38,39,43,48,49,64−66] Given that pyruvic acid processing in the atmosphere is dominated by photolysis,[18,26] it is necessary to develop a kinetic and mechanistic understanding of this chemistry in the wide variety of environments in which pyruvic acid is found. Because of its relevance to atmospheric chemistry and seeming sensitivity to reaction conditions, investigation of the aqueous photolysis of pyruvic acid, which progresses through triplet and radical chemistry to produce oligomeric products, has been revived,[18,40,42] yet, similar attention to its gas-phase

counterpart has not received similar recent attention. Nevertheless, as the gas-phase photolysis of pyruvic acid is expected to dominate over the aqueous photolysis as a sink for pyruvic acid under most atmospheric conditions,[14,18] a deeper fundamental understanding of this chemistry is essential.

Early literature on the photochemistry of pyruvic acid vapor characterized its photolysis under low overall pressures (less than 150 Torr) and high temperatures (~350 K), using narrowband radiation ($\lambda \leq 366$ nm).[39,48,67] These studies observed a quantum yield of about 1.0 for pyruvic acid loss upon photon absorption and identified products including CO_2 (~100% yield) and acetaldehyde (45−80% yield).[39,48] In considering the likely photochemical mechanisms at play, direct bond cleavage is often the most common form of photolysis. However, most of these pathways for pyruvic acid are inaccessible in the troposphere, requiring wavelengths of light less than 250 nm.[59] The one atmospherically feasible bond fission pathway, which can be achieved with radiation less than 340 nm, is breaking of the carbon−carbon bond between the keto and acid functional groups ($CH_3C(O)COOH \rightarrow CH_3\,^{\bullet}CO + {}^{\bullet}COOH$).[59] Never-theless, the most energetically favorable mechanism for the photolysis of gas-phase pyruvic acid, and the most direct pathway to CO_2 and acetaldehyde, requires hydrogen atom transfer and C−C bond cleavage, progressing through a five-membered, cyclic transition state.[39,59,60] Scheme 1 outlines this decarboxylation process to form methylhydroxycarbene, which eventually isomerizes into acetaldehyde.[39,61,68,69] This photochemical

Scheme 1. Primary Mechanism[a] for the Gas-Phase Photolysis of Pyruvic Acid, Yielding CO_2 and Acetaldehyde[39]

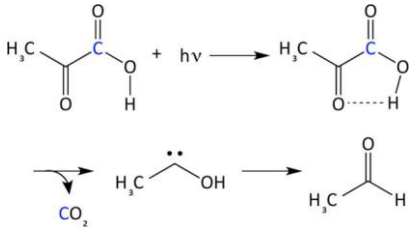

[a]The blue carbon represents the ^{13}C in labeled experiments.

[39,48,59,61]

In addition to the low-pressure work, three previous studies have investigated the photolysis of gas-phase pyruvic acid in air at atmospheric pressure (760 Torr). The first, by Grosjean in 1983,[47] photolyzed 330 ppb of pyruvic acid in a 4 m^3 Teflon chamber, using solar radiation as the light source.[47] Grosjean detected acetaldehyde and formaldehyde, noting that CO_2 is also a known major product.[47] In 1992, Berges and Warneck[46] performed an experiment under similar conditions, but with 50−100 ppm pyruvic acid and irradiation at 350 nm.[46] While they find a smaller quantum yield than the low-pressure laboratory studies ($\Phi = 0.85$), they do report similar product yields of acetaldehyde ($\Phi = 0.48$) and CO_2 ($\Phi = 1.27$). They also identify additional products, including acetic acid ($\Phi = 0.14$) and trace amounts of CO and CH_4.[46] A later analysis using a smog chamber also detected acetaldehyde, acetic acid, and CO, as well as formic acid and formaldehyde, but found lower pyruvic acid photolysis quantum yields of $\phi = 0.43$ and $\phi = 0.21$. These results are summarized in Mechanisms of Atmospheric Oxidation of the Oxygenates.[12,70,71]

Comparing the laboratory, low-pressure studies to results from experiments performed near atmospheric pressure, it is clear that new products are generated from pyruvic acid photolysis at higher pressures, where the reported quantum yields are highly variable. Further, the pressure dependent photolysis of other compounds with carbonyl functionality necessitates a systematic study of the effect of pressure on the photolysis of pyruvic acid.[15−17,72,73] In this fundamental study, we photolyze 0.05−0.9 Torr of pyruvic acid at room temperature (295 K) with 0−600 Torr of either nitrogen or air. The quantum yields and products are examined as a function of pyruvic acid concentration, total pressure, and the presence of oxygen, in order to characterize the sensitivity of gas-phase pyruvic acid photolysis to these variables.

II. EXPERIMENTAL SECTION

Photolysis of gas-phase pyruvic acid was investigated to deduce the effect of pyruvic acid concentration, total pressure, and the presence of oxygen on the decomposition rate and resulting products. Photolysis reactions were performed in an unmixed crossed glass cell to allow for concurrent sample irradiation and chemical analysis (Figure 1). To simulate the solar spectrum, we used a broadband light source (Newport 450 W Xe arc lamp) with a Pyrex window to attenuate UV-radiation below 290 nm (for spectrum see Figure 2). The lamp spectrum was recorded with a spectroradiometer (International Light, RPS900 Wise-band Rapid Portable Spectroradiometer) in absolute irradiance mode, and NO_2 actinometry was used to verify the quantification of the flux through the photochemical cell (see the Supporting Information for details of NO_2 actinometry).[8,74−76] Figure 2 shows our lamp spectrum and its overlap with the pyruvic acid UV cross-section, along with the solar flux near Earth's surface (see Figure S1 for full spectra).[77] The overlap of the actinic flux with our lamp spectrum clearly demonstrates the distribution of wavelengths in the region of the pyruvic acid absorption spectrum in the cell are very similar to those available in the troposphere, validating the atmospheric relevance of this study.

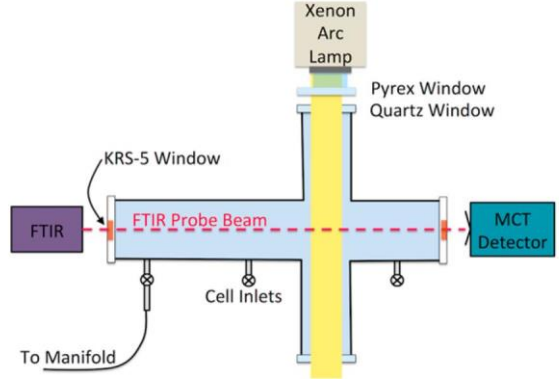

Figure 1. Crossed photochemical reaction vessel with photolysis and spectroscopic chambers. A collimated xenon arc lamp is directed through a Pyrex window to initiate photolysis with broadband, UV−visible radiation ($\lambda > 290$ nm). The concentration of pyruvic acid and its photoproducts are monitored in situ by FTIR.

Contents of the cell were monitored in situ by the external beam of a Bruker IFS-66v/s FTIR spectrometer, which was

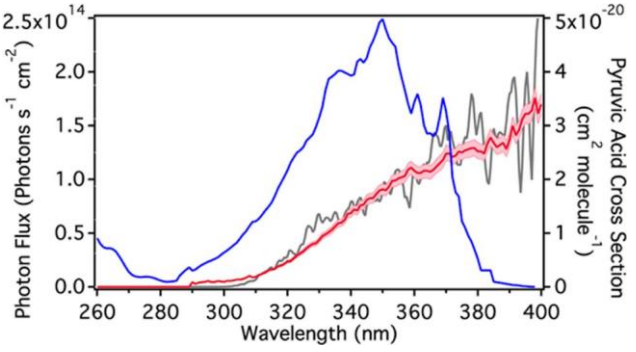

Figure 2. Lamp flux inside the cell (red) and its overlap with pyruvic acid's ultraviolet absorption cross-section (blue, reproduced from Sander et al.).[78] The pink shaded regions indicate the expected error in our quantification of the lamp photon flux. The gray trace represents the solar spectrum near Earth's surface to specify the similar distribution of wavelengths between our lamp and the actinic flux. The solar data was reproduced from Rottman and Woods (1991) but scaled for comparison.[77]

collected by a liquid nitrogen cooled MCT detector. FTIR spectra of the reacting mixture were taken every 5 min and analyzed using the MATLAB software, Main Polwin, which was developed at CEAM (Spain). It is based on a linear square fitting routine modified to improve the filtering process to remove baseline and broad absorptions of unknown compounds. This software compares standardized spectra, collected with the same apodization function (Happ-Genzel) and resolution (0.5 cm^{-1}) that we chose for our measurements, with the experimental spectra at each time step to determine the contribution of each chemical component. The program is run over at least five wavenumber ranges, to span the region from 760 to 3600 cm^{-1}, with each standardized spectrum added only after visual identification in the experimental spectra. The concentration of each species is then calculated from averages of the model output (ratios of a given products standardized spectrum to the absorption it contributes to each experimental FTIR spectra) over each wavenumber range and Beer's law.

Pyruvic acid (98%) was obtained from Sigma-Aldrich and distilled under reduced pressure before use. Reagents for the photolysis of labeled pyruvic acid include $CH_3C(O)^{13}COOH$ (≥99 atom % ^{13}C, ≥ 99% (CP), Sigma-Aldrich) and $CH_3{}^{13}COOH$ (≥99 atom % ^{13}C, Sigma-Aldrich). Before each experiment, pyruvic acid was degassed with at least nine freeze−pump−thaw cycles and heated to 30 °C while pulling vacuum for 5 min to remove excess water. It was then vaporized into the evacuated cell at room temperature (~22 °C) to a partial pressure of approximately 0.05, 0.3, or 0.9 Torr and balanced with nitrogen (Airgas, Ni UHP300) or synthetic air (Airgas, Ai Z300) to the desired pressure. Dark decays before photolysis show no reaction of pyruvic acid prior to irradiation. Addition-ally, some experiments were left in the dark for up to an hour following final light exposure. No increase of any product, nor decrease in pyruvic acid, was observed during this final dark period, and, therefore, the products we report must be directly related to photolysis.

An MSK baratron capacitance manometer (Type 626) was used to monitor pressure in the cell, which varied between 0 and 600 Torr depending on the experiment. Because of our small, unmixed photolysis reactor, care must be taken to ensure that gas diffusion throughout the cell is not competing with the decay of pyruvic acid. Experiments were performed with alternating dark and light intervals, and pyruvic acid decay was instantaneous upon irradiation at all pressures. Furthermore, no additional decrease in pyruvic acid occurred in the dark following photolysis. There is no indication in the data presented here that competition between diffusion and the photochemical decay of pyruvic acid is occurring under our reaction conditions. Nevertheless, because of the size of our cell and the slow photolysis of pyruvic acid near atmospheric pressure, the reported values in this work's highest-pressure experiments (600 Torr) are shown to indicate the continuation of a trend, but are not meant for further quantitative analysis.

III. DATA ANALYSIS

Here, we sought to determine the photolysis quantum yield for pyruvic acid as a function of pressure. This was accomplished by measuring the J-value, or first-order photochemical rate constant, at a variety of pressures and subsequently deriving the quantum yield from eq 1

$$J = \int_{\lambda_1}^{\lambda_2} d\lambda\, F(\lambda)\sigma(\lambda)\phi(\lambda) \quad (1)$$

where F is the photon flux, σ is the molecular cross section, and ϕ is the quantum yield.

To evaluate the J-value, the decay of pyruvic acid during dark and light intervals was characterized for each experiment. Pyruvic acid exhibited variable non-negligible wall losses in the dark, which were quantified by measuring pyruvic acid's rate of decay during alternating 30 min dark and light intervals. We approximate the dark decay as a first order process in which pyruvic acid irreversibly sticks to the wall with the rate constant k_d (s^{-1}) (eq 2).

$$[PA] = [PA]_0\, e^{-k_d t} \quad (2)$$

The J-value was determined from the overall loss rate for pyruvic acid during the light cycles, accounting for both the dark decay and photolysis simultaneously with the exponential expression,

$$[PA] = [PA]_0 e^{-(k_d + J)t} \quad (3)$$

For each cycle, we found k_d from the loss of pyruvic acid during the dark interval (eq 2), and then extracted J for the following photolysis period by fitting the data to eq 3. Figure 3 shows one example of the decay of pyruvic acid with the determined exponential curves. This method reproduced the data well for all experiments covered in this work, evidence that the primary loss mechanism for pyruvic acid in the cell was a result of unimolecular photolysis, as opposed to secondary chemistry.

Finally, average quantum yields were calculated for pyruvic acid from the determined J-value at each pressure and eq 1. It is important to note that we do not measure wavelength dependent J-values and therefore cannot determine ϕ(λ). What we report is an average quantum yield over the wavelengths of light for which pyruvic acid absorbs in our setup (~290−380 nm, Figure 2), and corresponds to excitation of S_1. Calculated quantum yields are tabulated in Table S1 and depicted in Figure 4. For each pressure and concentration, a minimum of two experiments and six dark/light cycles were analyzed and included in the overall reported ϕ_{Avg}. Error bars in Figure 4 were determined from calculated standard deviations of the measured J-values for pyruvic acid and for NO_2, which were propagated through the quantification of the photon flux in the cell, to determine the quantum yield uncertainty. Though the reported quantum yields include a range

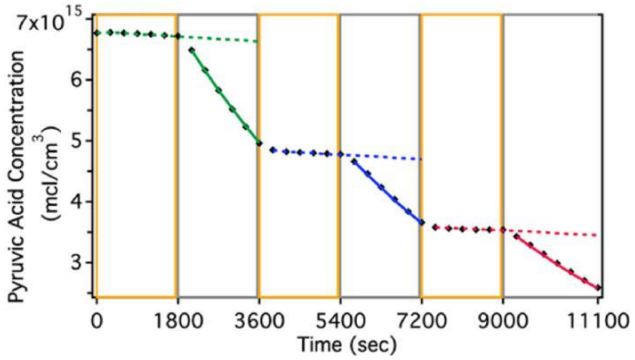

Figure 3. Example photolysis experiment of 0.22 Torr of pyruvic acid and 30 Torr of nitrogen, with three dark/light cycles. Gray boxes indicate dark conditions while yellow boxes represent photolysis periods. The black dots are experimental data. The dotted lines are the resulting fits to pyruvic acid in the dark, in the form of eq 2, and the solid lines are the fits to pyruvic acid during photolysis, in the form of eq 3.

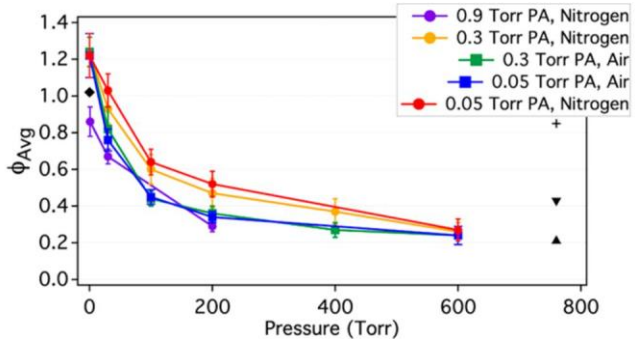

Figure 4. Quantum yields for the photolysis of pyruvic acid as a function of total pressure. Black markers indicate results from the previous studies: (♦) Vesley and Leermakers (1964),[39] (+) Berges and Warneck (1992),[46] and (▼, June) and (▲, October) Winterhalter et al. (2001).[70]

of wavelengths, given the good agreement between our lamp spectrum and the solar spectrum, they are representative of the average quantum yields expected for pyruvic acid in the atmosphere under dry conditions.

IV. ELECTRONIC STRUCTURE OF PYRUVIC ACID

Before discussing our results, we provide an overview of the energetic landscape of pyruvic acid, determined from the existing body of literature, in order to outline the photophysics relevant to the photochemistry of pyruvic acid. Figure 5 gives a qualitative overview of its electronic structure, compiled from previously published computational and laboratory studies.[39,48,59−61] There are two nearly isoenergetic conformers of pyruvic acid (Tc and Tt), which differ in their hydrogen bonding. We focus on the Tc conformation, which has a hydrogen bond between the acidic hydrogen and keto functional group and is therefore the more stable of the two conformers (Figure 5).[61,79,80]

The photolysis of pyruvic acid begins with absorption of a photon near 350 nm, which excites the molecule to S_1 through an $n-\pi^*$ transition, as shown in Figure 5, process A.[39,48,81] From here, a variety of different photophysical and photochemical processes can occur. Fluorescence, internal conversion, and/or vibrational relaxation (process B) would steer pyruvic acid back toward the ground state. Intersystem crossing from the S_1 state into the T_1 state may also occur. If the excitation is significant enough to overcome the barriers in S_1, the molecule could proceed along the S_1 surface to form products. However, a 2014 computational study by Chang et al. located a conical intersection between S_0 and S_1.[59] Internal conversion through the conical intersection would create a vibrationally hot molecule in S_0 that may continue toward decarboxylation on the S_0 surface or return to pyruvic acid.[59] Other photolysis pathways may also come from pyruvic acid molecules in the Tt conformation, which have a trans COOH arrangement, as there is an increase upon irradiation in the fraction of Tt pyruvic acid in the S_1 state.[79,80]

Previous laboratory studies are not conclusive regarding the state from which the mechanism outlined by Scheme 1 occurs, or whether a triplet surface is involved.[39,48,67] Both Vesley and Leermakers (1963)[39] and Yamamato and Back (1983)[48] conclude that lack of quenching from oxygen likely rules out T_1 as a significant player in the gas-phase photolysis.[39,48] However, if the lifetime of the excited state is significantly shorter than collision times, the absence of an oxygen effect does not inform this subject.[39] In fact, according to Chang et al.,[59] the T_1 surface, possibly accessed via the conical intersection, may be an additional source of methylhydroxycarbene and CO_2.[59] Assuming the majority of pyruvic acid does react on a singlet surface, as these studies speculate, the existing literature is unable to define whether it occurs in the first excited (S_1) or ground state (S_0). Yamamoto and Back (1983) imply the major process is on the S_1 surface, but they do not explicitly consider the possibility of decarboxylation on S_0.[48] Experimental and computational work regarding vibrational overtones of pyruvic acid demonstrate that S_0 chemistry can yield CO_2 and acetaldehyde.[39,48,59,56−58,60] While we do not rule out the possibility of some triplet state involvement in the chemistry, the most probable [58,68] photolysis pathway following excitation to S_1 is for pyruvic acid to proceed via intersystem crossing through the conical intersection and decarboxylate in S_0 to form ground state methylhydroxycarbene (mHC:CH2, the ground state of CH3COH) in a singlet[59] and CO2. Methylhydroxycarbene then must overcome a significant barrier (~10 kJ/mol[79]) to form the observed final product, acetaldehyde. We note that the pathway to form methylhydroxycarbene in S_0, combined with the barrier to the isomerization reaction that forms acetaldehyde, suggests that it could have a longer lifetime than expected, allowing it to participate in favorable bimolecular reactions.

V. DISCUSSION

V.A. The Kinetics of the Photolysis of Gas-Phase Pyruvic Acid.

Figure 4 shows the average photolysis quantum yields (ϕ_{Avg}) determined for initial pyruvic acid pressures of 0.05 and 0.3 Torr as a function of pressure of air and nitrogen from 0 to 600 Torr. Because broadband radiation was used for this experiment, our quantum yields are an average over the entire S_1 transition (~290−380 nm, Figure 2).

For the photolysis of 0.3 Torr of pyruvic acid with no buffer gas, we measure $\phi_{Avg} = 1.24 \pm 0.08$, which is an increase from the previously published low-pressure quantum yield of 1 by Vesley and Leermakers (1964),[39] and indicates some radical chemistry in our system. Vesley and Leermakers (1964),[39] however, used monochromatic radiation of 360 nm, while we use a broadband solar simulator with radiation reaching as low as 300 nm. There is previous evidence the direct bond cleavage channel, creating $CH_3^{\bullet}CO$ and $^{\bullet}COOH$, can account for approximately 40% of pyruvic acid loss when it is irradiated with 350 nm radiation;[46] although, computational studies have reported the threshold may be closer to 340 nm.[59] Nevertheless, while there is substantial

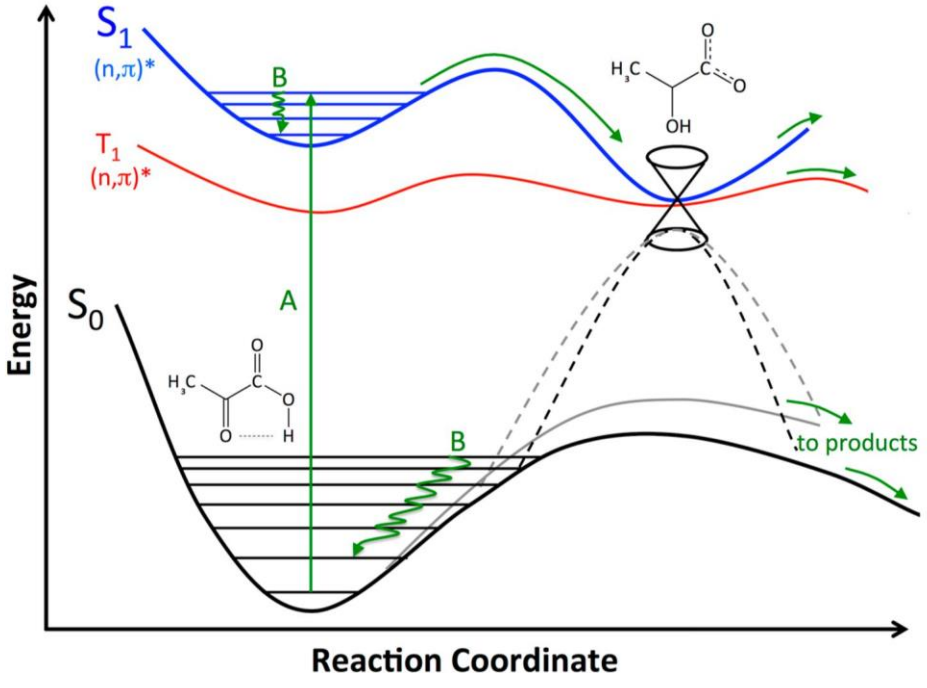

Figure 5. Qualitative electronic structure diagram for pyruvic acid, as described in Chang et al. (2014),[59] with important photophysical and photochemical processes indicated by green arrows. UV radiation can excite pyruvic acid from its ground state, shown in the Tc conformer, to the S_1 state (A). Vibrational relaxation (B) could inhibit the molecules ability to overcome barriers to decarboxylation.

light in our system for some bond fission to occur, it is likely this pathway accounted for much less of the pyruvic acid decay in Vesley and Leermaker's lower energy experiment. Further, acetaldehyde photolysis to $^{\bullet}CH_3$ and $^{\bullet}CHO$ is possible with $\lambda < 330$ nm (see also section V.B), which may act as another small source of radicals in our system.[15,59] Once created, these radicals, which will be higher in concentration in our system than in the Vesley and Leermakers experiment, can initiate radical reactions that consume more than one pyruvic acid molecule per photon absorbed by pyruvic acid, resulting in a quantum yield greater than one.

As the pressure of buffer gas is increased from 0 Torr, the quantum yield decreases. While this effect is observed for experiments performed in both nitrogen and air, the quantum yields in air were consistently lower than their counterparts in nitrogen, particularly between 30 and 200 Torr. Additionally, the quantum yield decreases as the initial concentration of pyruvic acid is increased. This is the first report of a clear effect of pressure on the photolysis quantum yield of gas-phase pyruvic acid. Nevertheless, there are studies of other carbonyl molecules, including acetaldehyde and acetone, that exhibit a similar decrease in quantum yield with increasing buffer gas pressures.[15−17,72,82]

The current literature regarding quantum yields for pyruvic acid photolysis at higher pressures is inconsistent. Vesley and Leermakers (1963)[39] and Yamamoto and Back (1985)[48] studied the photolysis in pressures up to 150 Torr and found no reduction in ϕ; however, they used higher pyruvic acid concentrations and temperatures than our experiments. Conversely, all of the quantum yields measured from experi-ments conducted at pressures near 760 Torr to date have been smaller than 1; however, they span a wide range from $\phi = 0.85$ to $\phi = 0.21$.[13,46,70,78] The variability between these measurements could be due to differences in water content, pyruvic acid concentration, and/or the light source used, as they are not consistent between the different studies. Our results, which give a quantum yield of $\phi = 0.24 \pm 0.05$ for the photolysis of pyruvic acid in 600 Torr of air, agree with the low end of these previously reported values.[46,70,78]

We conducted a Stern−Volmer analysis to explore the possibility of collisional deactivation as the mechanism for the decrease in quantum yield. If only the singlet state is actively quenched, we expect a linear relationship between $1/\phi$ and [M]; however, if both the singlet and triplet states are accessible and quenched, a Stern−Volmer analysis will result in a nonlinear curve.[16,17,83] According to the known primary pathway for decarboxylation (Scheme 1), the mechanism begins by exciting pyruvic acid (PA) to a reactive singlet state (PA(S)*, eq 4a), which could be in either S_1 or S_0. PA(S)* then decarboxylates to form CO_2 and methylhydroxycarbene (eq 4b). We add the possibility that collision with the buffer gas, M, returns PA(S)* to an unreactive form of pyruvic acid, PA (eq 4c).

$$PA + h\nu \rightarrow PA(S)^* \qquad k_1 \qquad (4a)$$

$$PA(S)^* \rightarrow CO_2 + CH_3COH \qquad k_{dS} \qquad (4b)$$

$$PA(S)^* + M \rightarrow PA + M \qquad k_{qS} \qquad (4c)$$

Though a majority of the products are expected to be produced on the singlet surface, there is some computational evidence for triplet involvement.[59] We therefore include the possibility that pyruvic acid can intersystem cross into the triplet regime, where it will either decarboxylate or be quenched (eq 4d−f).

$$PA(S_1)^* \rightarrow PA(T_1)^* \qquad k_{ISC} \qquad (4d)$$

$$PA(T)_1^* \rightarrow CO_2 + CH_3COH \qquad k_{dT} \qquad (4e)$$

$$PA(T)_1^* + M \rightarrow PA + M \qquad k_{qT} \qquad (4f)$$

If this mechanism describes the most important processes involved in the loss of pyruvic acid, a plot of $1/\phi_{measured}$ versus [M] will produce a curve corresponding the equation:

$$\frac{1}{\phi_{measured}} = \frac{A\,[M]^2 + B\,[M] + C}{\phi_0\,(\alpha[M] + \beta)} \quad (5a)$$

where ϕ_0 is the quantum yield with no buffer gas, $\phi_{measured}$ is the measured quantum yield at each pressure, and A, B, C, α, and β are a combination of the six rate constants from eq 4 (see Supporting Information, section 3).[84] If quenching only occurs in the singlet state, eq 5a reduces to the linear equation

$$\frac{1}{\phi_{measured}} = \gamma\,[M] + \zeta \quad (5b)$$

where γ and ζ are new combinations of the five remaining rate constants. Because there are more rate constants than variable coefficients for both eq 5a and eq 5b, we cannot extract information about the individual rate constants and therefore do not reproduce the whole equations or values for constants here. See Supporting Information, section 3, for full derivation and constant values determined by regression analysis.

Figure 6 shows $1/\phi_{measured}$ versus [M] for the photolysis of 0.05 Torr of pyruvic acid in air and in nitrogen (see Figure S2 for

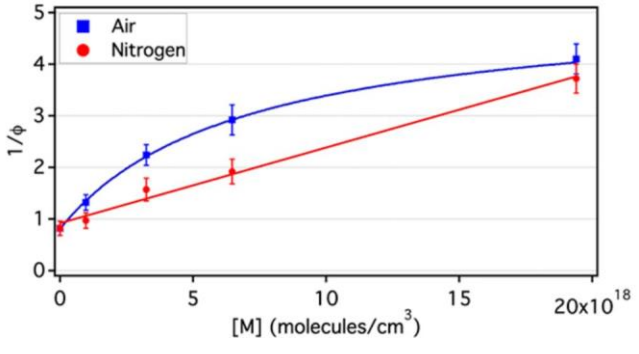

Figure 6. Stern−Volmer Plot for 0.05 Torr of pyruvic acid with M = N_2 (red) and 0.05 Torr pyruvic acid with M = air (blue). The data for the photolysis of pyruvic acid in nitrogen fits a line eq 5b, while the data taken in air fits the form of eq 5a. See Supporting Information, section 3, for constant values from regression analysis.

0.3 and 0.9 Torr Stern−Volmer plots). The quantum yields from photolysis reactions performed in air fit the shape of eq 5a well (R^2 = 0.9997), indicating the triplet state is slightly accessible and both the singlet and triplet states are quenched by O_2. Conversely, the quantum yields from photolysis reactions performed in nitrogen exhibit linearity (R^2 = 0.9901). This result indicates that, when M = N_2, the decrease in quantum yield with increasing pressure is due primarily to collisional deactivation of the singlet state of pyruvic acid, while the triplet state is not effectively quenched by nitrogen. The Supporting Information (section 3) gives the coefficients for the lines, determined in MATLAB.

Upon inspection, there are a few reasons we observe a linear Stern−Volmer trend in nitrogen but a curved one in air. First, collision-induced electronic deactivation of pyruvic acid from S_1 to S_0 is improbable.[48] Therefore, the singlet state quenching is likely due to vibrational deactivation, prohibiting pyruvic acid from accessing the final decarboxylation pathway in S_0. Vibrational deactivation is also consistent with the decreasing quantum yield with increasing pyruvic acid concentration, as pyruvic acid is expected to be more efficient than O_2 or N_2 in the quenching of PA* given its size and resonant frequencies. However, the barrier to reaction in the triplet state is expected to be low,[59] so its quenching would require electronic deactivation to the singlet ground state, a forbidden transition and significantly slower process in nitrogen. On the other hand, the presence of oxygen, an efficient quencher of triplet states,[83] allows for rapid interconversion from $PA(T_1)^*$ to $PA(S_0)$, resulting in quenching of two states and the curved trend in air.

This Stern−Volmer analysis shows that the triplet state of gas-phase pyruvic acid is slightly accessible, but that most pyruvic acid decays from a singlet manifold. The small reduction in quantum yield in air compared to nitrogen is due to triplet quenching made possible by the presence of oxygen. Although, as is clear from Figure 4, this decrease in rate due to triplet quenching is much less than that from singlet collisional deactivation, indicating that only a few trajectories in the photolysis of pyruvic acid actually proceed on the triplet surface. Previous laboratory studies did not observe an effect of air, and therefore ruled out the triplet state as a major player in this reaction.[39,48] The T_1 effect we discern is minor, and therefore, our result agrees with previous conclusions that a majority of pyruvic acid decay is due to singlet chemistry.

V.B. Products from Gas-Phase Pyruvic Acid Photolysis. Table 1 lists average percent yields determined here for the products from pyruvic acid photolysis as a function of pressure and also includes those available from previous studies of pyruvic acid photolysis at 760 Torr.[46,70,71] FTIR spectra confirming the identification of each product, as well as experimental data for products for an example experiment, are shown in the Supporting Information (Figures S3−S7). In agreement with the literature to date, the major products under all conditions in this work are carbon dioxide and acetaldehyde, indicating

Scheme 1 is indeed the primary photolysis pathway.[39,48,59,60]

Earlier studies of the photolysis of pyruvic acid measured yields of 45−80% for acetaldehyde and 100−127% for CO_2.[39,46,48] Our results are consistent with these values, with acetaldehyde percent yields ranging between 40% and 70%, while the carbon dioxide yields are generally much higher, between 80% and 140%. Carbon dioxide yields in excess of acetaldehyde, and above 100%, are consistently reported in previous works, and are discussed briefly below.

Many minor products are also identified in these experiments (Table 1). Of these, formaldehyde,[47,70,71] formic acid,[70,71] methane,[39,46] methanol,[46] carbon monoxide,[39,46,70,71] and acetic acid[46,70,71] have been characterized in previous studies, though no paper includes them all. The yields in Table 1 are relatively consistent with the literature to date in that they are similar to previously published yields for each product in the respective studies. However, acetic acid has never before been observed in the low-pressure laboratory studies of pyruvic acid photolysis. Further, our pressure specific data highlights an interesting new trend in the acetic acid percent yields they increase with increasing pressure of buffer gas. This effect is amplified in air, resulting in a maximum acetic acid yield of 15% when pyruvic acid is photolyzed in 600 Torr of air. This behavior indicates there could be multiple pathways leading to acetic acid. A recent computational paper provides some insight into one possible mechanism to form acetic acid directly from the photolysis of pyruvic acid.[60] Da Silva (2016)[60] highlights an energetically feasible reaction coordinate, which proceeds through a lactone transition state to create CO and acetic acid. He predicts that it

Table 1. Average Final Percent Yields[a] of Products Calculated from the Photolysis of Pyruvic Acid[b]

$p_{buffer\ gas}$		$p_{pyruvic\ acid}$	product yields (%) for the photolysis of gas-phase pyruvic acid								
(Torr)	buffer gas	(Torr)	CO_2	CO	^{13}CO	$CH_3CH(O)$	$CH_3C(O)OH$	HCH(O)	CH_4	CH_3OH	HC(O)OH
0.0	none	0.3	49 ± 3	4.0 ±0.3	–	53 ± 3	2.5 ± 0.2	0.50 ± 0.03	1.01 ± 0.06	1.9 ± 0.2	0.68 ± 0.05
0.0	none	0.05	85 ± 16	10 ±2	–	49 ± 9	3 ± 2	2.0 ± 0.7	1.7 ± 0.5	4 ± 1	1.4 ± 0.6
30.0	air	0.3	89 ± 9	3.7 ±0.4	–	56 ± 6	4 ± 1	2.2 ± 0.9	0.08 ± 0.04	5 ± 4	1.0 ± 0.2
30.0	air	0.05	103 ± 6	4.8 ±3	–	61 ± 3	4.7 ± 0.4	3.5 ± 0.2	0.34 ± 0.09	1.2 ± 0.4	0.7 ± 0.1
30.0	nitrogen	0.3	88 ± 10	3.8 ±0.6	–	56 ± 6	3.1 ± 0.2	0.73 ± 0.09	0.19 ± 0.03	5.4 ± 0.5	0.69 ± 0.05
30.0	nitrogen	0.05	98 ± 6	4.0 ±0.2	–	60 ± 4	0.6 ± 0.1	0.8 ± 1	–	5.0 ± 0.6	0.9 ± 0.86
30.0	nitrogen	0.3*	–	1.4 ±0.1	1.4 ± 0.1	41 ± 3	1.2 ± 0.2	0.75 ± 0.06	0.13 ± 0.08	5.5 ± 0.4	0.3 ± 0.1
100.0	air	0.3	127 ± 26	5 ±1	–	65 ± 14	9 ± 2	5 ± 1	0.10 ± 0.03	2.3 ± 0.6	2.9 ± 0.8
100.0	air	0.05	139 ± 23	6 ±1	–	69 ± 12	7 ± 1	6 ± 1	–	1.2 ± 0.6	1.9 ± 0.3
100.0	nitrogen	0.3	116 ± 28	4 ±1	–	62 ± 14	3.6 ± 0.8	1.3 ± 0.3	–	10. ± 2	0.9 ± 0.2
100.0	nitrogen	0.05	129 ± 35	5 ±1	–	73 ± 21	2.4 ± 0.6	1.8 ± 0.5	–	8 ± 3	0.8 ± 0.6
200.0	air	0.3	108 ± 28	4 ±1	–	53 ± 13	11 ± 3	5 ± 1	0.02 ± 0.02	2 ± 1	5 ± 2
200.0	air	0.05	120 ± 26	5 ±2	–	60 ± 14	10 ± 2	7 ± 2	0.15 ± 0.22	1.1 ± 0.3	2.5 ± 0.9
200.0	nitrogen	0.3	122 ± 45	4 ±1	–	60 ± 17	5 ± 2	1.6 ± 0.8	–	12 ± 5	1.3 ± 0.4
200.0	nitrogen	0.05	109 ± 24	4 ±1	–	61 ± 14	4 ± 2	1.9 ± 0.9	–	8 ± 3	0.8 ± 0.3
400.0	air	0.3	99 ± 14	3.3 ±0.5	–	45 ± 6	12 ± 2	5.6 ± 0.8	–	2.2 ± 0.3	3.4 ± 0.6
400.0	nitrogen	0.3	96 ± 17	3.0 ±0.5	–	49 ± 7	4.4 ± 0.6	1.9 ± 0.3	–	11 ± 2	
600.0[c]	air	0.3	110 ± 25	3.4 ±0.7	–	46 ± 11	18 ± 6	7 ± 1	–	4 ± 2	5 ± 2
600.0[c]	air	0.05	137 ± 26	5 ±2	–	51 ± 16	15 ± 4	10. ± 3	0.19 ± 0.08	2.3 ± 0.7	2.7 ± 0.6
600.0[c]	nitrogen	0.3	115 ± 17	3.5 ±0.5	–	51 ± 9	9 ± 2	4.12 ± 0.9	–	14 ± 3	1.9 ± 0.5
600.0[c]	nitrogen	0.05	108 ± 18	4.0 ±0.5	–	53 ± 10	6.4 ± 0.73	6.0 ± 0.8	–	4.2 ± 0.6	0.7 ± 0.1
760.0	air[d]	~0.04	127 ± 18	<13		48 ± 1	14 ± 3			<4	
760.0	air[e]			8 ±3		27 ± 5	11 ± 2	8 ± 3			3 ± 2

[a]Final product concentration/amount of pyruvic acid reacted. [b]Between 56% and 98% of carbon is recovered for the contributing photolysis reactions. Starred pyruvic acid pressure designates isotopically labeled pyruvic acid ($CH_3C(O)^{13}COOH$) was used as the reagent. [c]As noted in section II, these values are shown to indicate the continuation of a trend, but are not meant for further quantitative analysis. [d]Percent yields published by Berges and Warneck (1992).[46] [e]Percent yields from photolysis experiments in the EUPHORE chamber.[70,71]

could account for 1−4% of pyruvic acid loss under atmospheric conditions (Scheme 2).[60]

With no buffer gas, photolysis of pyruvic acid in our experiments produces an acetic acid yield (~2.5−3%) compatible with da Silva's (2016)[60] calculations, indicating the acetic acid in our low-pressure experiments could indeed be a result of Scheme 2. Though CO is in excess with respect to acetic acid at low pressures, at least part of it can be attributed to the photolysis of acetaldehyde (discussed below).[82] In order to test this mechanism, we examine the products from the photolysis of 0.3 Torr of labeled pyruvic acid ($CH_3C(O)^{13}COOH$) balanced with 30 Torr of nitrogen (yields corresponding with this experiment are denoted in Table 1 with the starred pyruvic acid partial pressure). We chose to use pyruvic acid labeled at the acidic carbon because, if the lactone chemistry were occurring, the resulting carbon monoxide would be labeled and easily distinguishable from ^{12}CO with FTIR. Schemes 1 and 2 track the isotopically labeled carbon in blue, yielding either $^{13}CO_2$ or ^{13}CO, respectively (Schemes 1 and 2). These experiments were difficult to quantify; however, they do support the lactone mechanism. The detected acetic acid and acetaldehyde were unlabeled, and no unidentified peaks in the FTIR spectrum corresponded to $CH_3{}^{13}COOH$ (Figure S8). Further, although both CO and ^{13}CO were produced, ^{13}CO was present in approximately equal concentration to acetic acid (Table 1). While these results are not unequivocally conclusive, they are consistent with the mechanism described by Da Silva.[60]

At this point, it is instructive to examine the ratio of acetic acid to CO at the end of each pyruvic acid photolysis as a function of the total pressure (Figure 7). The ratio $[CH_3COOH]/[CO]$ increases more quickly with increasing pressure of air than with increasing pressure of N_2, surpassing one at pressures as low as 30 Torr. This suggests there must be a second mechanism that

Scheme 2. Mechanism[a] for the Photolysis of Pyruvic Acid Yielding CO and Acetic Acid[60]

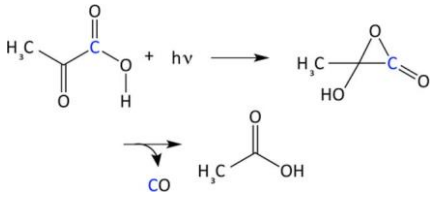

[a]The blue carbon represents the labeled carbon in the isotope experiments.

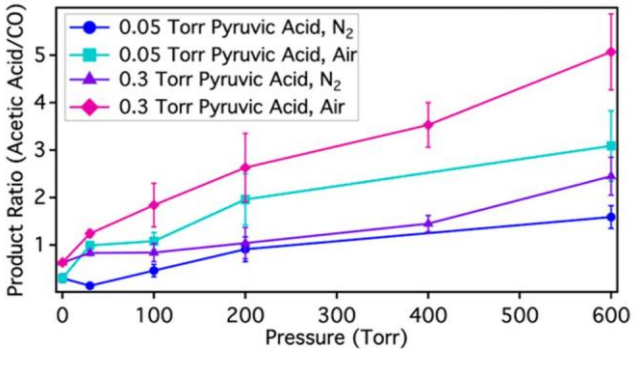

Figure 7. Final ratios of acetic acid to CO as a function of pressure for all initial pyruvic acid concentrations in both nitrogen and air.

produces acetic acid without also forming CO, likely involving oxygen. One possibility is a reaction between methylhydroxycarbene and O_2, which would decompose to yield HO_2 and CH_3CO. This radical pair could recombine to make peroxyacetic acid, which can photochemically decompose to CH_3CO_2 and OH, with the former going on to abstract a hydrogen atom to become acetic acid (see Figure S9, and section 4, in the Supporting Information for calculation details). There is only a weak overlap between the emission spectrum of our lamp and the absorption spectrum of peroxyacetic acid, and so this may not be the principal route by which the radical products would yield acetic acid. However, Berges and Warneck (1992)[46] provide evidence that CH_3CO, which can be formed either from the methylhydroxycarbene and oxygen reaction or from direct bond cleavage of pyruvic acid, can react with O_2 to give CH_3CO_3, which in turn reacts with HO_2 to give acetic acid and O_3. Table S2 contains the elementary reactions for this process, and demonstrates that this chemistry can explain not only the rising yield of acetic acid as the concentration of O_2 is increased, but also the observed formaldehyde and methanol.[78,85,86] Additionally, this scheme can produce more than one CO_2 molecule per pyruvic acid, so it may also account for the CO_2 yields greater than 100%.

For photolysis reactions performed in nitrogen, the ratio of acetic acid to CO increases much more slowly than those in air. It does not exceed 1 until 400 Torr. Compared to the photolysis in air, the growth of the acetic acid yield at higher pressures of nitrogen is more puzzling. It is possible the trend is an artifact of atmospheric oxygen leaking slowly into the nitrogen line during the experimental setup. While leak rates in the cell were less than 3 mTorr/min, it takes significantly longer to fill the cell to the higher pressures (>200 Torr), thus more oxygen may be getting into the reaction environment through the introduction of nitrogen and creating an artificial rise in acetic acid percent yield. Alternatively, there may be a third pathway responsible for this increase that comes from an excited state of pyruvic acid, possibly involving the Tt conformer, or a secondary reaction, to yield acetic acid without consuming O_2 or making CO. It is important to note that the carbon monoxide yield is consistently between 3% and 6% for all experiments at pressures of 30 Torr or greater (Table 1), where no acetaldehyde photolysis is observed. This is close to the amount of CO da Silva (2016)[60] estimates the lactone mechanism will produce, so some acetic acid at all pressures is likely generated from that decay pathway.

One possible source for some other minor products is the photolysis of acetaldehyde, which is known to decompose upon irradiation through three channels: eq 6a, 6b, and 6c.[15,82,87−89]

$$CH_3CHO + h\nu \rightarrow {}^{\bullet}CH_3 + {}^{\bullet}CHO \quad (6a)$$

$$CH_3CHO + h\nu \rightarrow {}^{\bullet}H + {}^{\bullet}CH_3CO \quad (6b)$$

$$CH_3CHO + h\nu \rightarrow CO + CH_4 \quad (6c)$$

There is, however, minimal flux from our lamp with the wavelengths necessary to excite acetaldehyde (230−340 nm), and its photolysis rate is known to decrease with increasing pressure;[15,82] therefore acetaldehyde photochemistry is expected to be minimal in a majority of our experiments, especially at higher pressures. Small amounts of methane (<2%) are observed only in the lowest pressure photolysis reactions, when the acetaldehyde photolysis rate is greatest. Thus, it is likely that methane, and corresponding amount of CO, is a result of the pathway in eq 6c. The radicals from eq 6a and eq 6b were not detected here, but are listed since their further chemistry could help explain other minor products. While the mechanism from the early literature on the gas-phase photolysis of pyruvic acid is clearly the major pathway, the minor products identified here, and their pressure dependence, signify additional noteworthy pathways, possibly involving multiple pyruvic acid conformers and/or electronic states.

VI. CONCLUSIONS

This work provides new fundamental insight into the kinetics of and products from the gas-phase photolysis of pyruvic acid. For all concentrations of pyruvic acid explored here, the photolysis quantum yield decreases as the total pressure of the system is increased. This study has also identified acetic acid as a product of photolysis in all pressures investigated. Acetic acid has not previously been detected in the low-pressure laboratory studies of pyruvic acid photolysis.[39,48,67] Furthermore, while the major products, acetaldehyde and CO_2, do not exhibit a pressure dependence, the yield of acetic acid relies strongly on pressure, in particular in air. As previously documented, the major products result from a five-membered, cyclic transition state that yields CO_2 and methylhydroxycarbene.[39,48,59,67] However, the pressure dependence of acetic acid observed here defines at least two additional pathways: one that generates CO and acetic acid via a lactone intermediate and another that involves a reaction with O_2.

Some possible mechanisms for the creation of acetic acid were suggested in sectionV.B, however, there are additional con-formers of pyruvic acid that could also contribute to chemistry occurring in these experiments.[61,79, 80] For example, all mechanisms outlined in this work begin from the more stable conformer of pyruvic acid, Tc, which has a hydrogen bond between the acidic hydrogen and ketone oxygen, as shown in Schemes 1 and 2. However, the Tt conformer has been seen to increase in concentration upon irradiation,[79,80] and may initiate chemistry not considered here. Though pyruvic acid is only a three-carbon molecule, there are many structures from and pathways by which photochemistry can proceed; here we consider only a few.

The results presented in this work have important consequences for pyruvic acid in the atmosphere. The pressure dependent photolysis quantum yield for pyruvic acid indicates the rate of removal via photochemical channels will have an altitude dependence in the troposphere. Given that this pressure effect is also found in acetone and acetaldehyde,[15 ,82] it is likely that other atmospherically relevant aldehydes and ketones may exhibit a similar effect and should be investigated. Further, the identification of acetic acid as a photolysis product is important to our understanding of atmospheric chemistry, as model studies show that our current knowledge of the sources and sinks of acetic acid in the environment is incomplete.[90−92] With concentrations on the order of 100 ppt, gas-phase pyruvic acid photolysis itself cannot explain the discrepancies; however, it presents a new class of mechanisms to be considered as possible pathways to form acetic acid.

Reed Harris et al. 2014[18] published a model study that compared the rates of pyruvic acid removal from several different sinks. The results suggested that the photolysis pathways in both the aqueous and gas phase, dominate over oxidation by OH, with the gas-phase photolysis being more efficient under most, though not all, conditions. The model, however, calculated the J-value for gas-phase pyruvic acid using an assumed quantum yield of 1.[18] Results presented here indicate the quantum yield is less than

8,12,93

The sensitivity of the photolysis of pyruvic acid to important atmospheric conditions, such as total pressure and concen-tration, has broader implications for research methods in atmospheric chemistry. Reactions need to be studied under atmospherically relevant conditions, as even small fluctuations in environment could have large ramifications on products and rates. This laboratory study provides a bridge[39,48,67] between the simulation chamber investigations to date[46,47] by systematically studying the photochemistry of pyruvic acid over a range of buffer gas pressures (0−600 Torr) and compositions (air and N_2). There are, however, conditions in the atmosphere that have not been explicitly studied and may be hard to reproduce in the laboratory. Although this study uses lower concentrations than previous efforts, pyruvic acid in the troposphere is found at even lower mixing ratios than in this work. Further, the small cell we use introduces wall processes and diffusion rates that become more competitive with decomposition via photolysis at pressures near 1 atm. Analysis in a large environmental simulation chamber would allow for conditions to remain highly controlled, for lower concentrations of pyruvic acid to be studied, and for the minimization of wall and diffusion effects. Future examination of the photolysis of gas-phase pyruvic acid in such a chamber would extend this data set to realistic atmospheric conditions.

ASSOCIATED CONTENT

* Supporting Information

Section 1 in the Supporting information contains figures of the full Xe arc lamp spectrum, Stern−Volmer plots for the photolysis of 0.3 and 0.9 Torr pyruvic acid, FTIR spectra identifying each product from Table 1, an example experiment showing growth of minor products, an FTIR spectrum indicating we identify unlabeled acetic acid from the photolysis of labeled pyruvic acid, and the Intrinsic Reaction Coordinate for the calculation of the abstraction of OH from CH_3COH, as well as tables containing ϕ_{Avg} and J values, the reactions and rate constants for the radical formation of acetic acid, and the numbers used to calculate the expected removal rates of pyruvic acid from the atmosphere via photolysis and reaction with OH. Sections 2−4 contain a description of NO_2 actinometry, a derivation of the Stern−Volmer equations used in the manuscript, and information regarding the calculation for the abstraction of OH from CH_3COH (PDF)

AUTHOR INFORMATION

Corresponding Author

*(V.V.) E-mail: Vaida@colorado.edu.

ORCID

Veronica Vaida: 0000-0001-5863-8056

Notes

The authors declare no competing financial interest.

ACKNOWLEDGMENTS

The authors wish to thank Dr. Mila Rodenas García for the development of Main Polwin as well as for sharing her expertise in using it. The EUROCHAMP-2 project (EC Contract No. 228335) is gratefully acknowledged for allowing the distribution of this software. Additionally, the authors recognize Russell J. Perkins and Jay A. Kroll for insightful discussion and assistance regarding the design and setup for the experiments published here. This work was supported by grants from the National Science Foundation (CHE 1306386 and CHE 1611107). A.E.R.H. also acknowledges funding from the National Science Foundation Graduate Research Fellowship under Grant No. DGE 1144083. Any opinion, findings, and conclusions or recommendations expressed in this material are those of the authors(s) and do not necessarily reflect the views of the National Science Foundation.

REFERENCES

(1) George, C.; Ammann, M.; D'Anna, B.; Donaldson, D. J.; Nizkorodov, S. A. Heterogeneous Photochemistry in the Atmosphere. Chem. Rev. 2015, 115 (10), 4218−4258.

(2) George, C.; D'Anna, B.; Herrmann, H.; Weller, C.; Vaida, V.; Donaldson, D. J.; Bartels-Rausch, T.; Ammann, M. Emerging Areas in Atmospheric Photochemistry; Springer-Verlag: Berlin and Heidelberg, Germany, 2014; Vol. 339.

(3) Rapf, R. J.; Vaida, V. Sunlight as an Energetic Driver in the Synthesis of Molecules Necessary for Life. Phys. Chem. Chem. Phys. 2016, 18 (30), 20067−20084.

(4) Vaida, V. Spectroscopy of Photoreactive Systems: Implications for Atmospheric Chemistry. J. Phys. Chem. A 2009, 113 (1), 5−18.

(5) Gligorovski, S.; Strekowski, R.; Barbati, S.; Vione, D. Environ-mental Implications of Hydroxyl Radicals (Center Dot OH). Chem. Rev. 2015, 115 (24), 13051−13092.

(6) Goldstein, A. H.; Galbally, I. E. Known and Unexplored Organic Constituents in the Earth's Atmosphere. Environ. Sci. Technol. 2007, 41 (5), 1514−1521.

(7) Atkinson, R.; Arey, J. Atmospheric Degradation of Volatile Organic Compounds. Chem. Rev. 2003, 103 (12), 4605−4638.

(8) Finlayson-Pitts, B. J.; Pitts, J. N. Chemistry of the Upper and Lower Atmosphere: Theory, Experiments and Applications; Academic Press: San Diego, CA, and London, 2000.

(9) Seinfeld, J. H.; Pandis, S. N. Atmospheric Chemistry and Physics: From Air Pollution to Climate Change, 2nd ed.; Wiley: Hoboken, NJ, 2006.

(10) Andreae, M. O.; Crutzen, P. J. Atmospheric Aerosols: Biogeochemical Sources and Role in Atmospheric Chemistry. Science 1997, 276 (5315), 1052−1058.

(11) Atkinson, R. Kinetics and Mechanisms of the Gas-Phase Reactions of the Hydroxyl Radical with Organic-Compounds under Atmospheric Conditions. Chem. Rev. 1986, 86 (1), 69−201.

(12) Mellouki, A.; Mu, Y. J. On the Atmospheric Degradation of Pyruvic Acid in the Gas Phase. J. Photochem. Photobiol., A 2003, 157 (2− 3), 295−300.

(13) Moortgat, G. K. Important Photochemical Processes in the Atmosphere. Pure Appl. Chem. 2001, 73 (3), 487−490.

(14) Epstein, S. A.; Nizkorodov, S. A. A Comparison of the Chemical Sinks of Atmospheric Organics in the Gas and Aqueous Phase. Atmos. Chem. Phys. 2012, 12 (17), 8205−8222.

(15) Warneck, P.; Moortgat, G. K. Quantum Yields and Photo-dissociation Coefficients of Acetaldehyde in the Troposphere. Atmos. Environ. 2012, 62, 153−163.

(16) Blitz, M. A.; Heard, D. E.; Pilling, M. J. Study of Acetone Photodissociation over the Wavelength Range 248−330 nm: Evidence of a Mechanism Involving Both the Singlet and Triplet Excited States. J. Phys. Chem. A 2006, 110 (21), 6742−6756.

(17) Salter, R. J.; Blitz, M. A.; Heard, D. E.; Pilling, M. J.; Seakins, P. W. Pressure and Temperature Dependent Photolysis of Glyoxal in the

355−414 nm Region: Evidence for Dissociation from Multiple States. Phys. Chem. Chem. Phys. 2013, 15 (17), 6516−6526.
(18) Reed Harris, A. E.; Ervens, B.; Shoemaker, R. K.; Kroll, J. A.; Rapf, R. J.; Griffith, E. C.; Monod, A.; Vaida, V. Photochemical Kinetics of Pyruvic Acid in Aqueous Solution. J. Phys. Chem. A 2014, 118 (37), 8505−8516.
(19) Horowitz, A.; Meller, R.; Moortgat, G. K. The UV-Vis Absorption Cross Sections of the Alpha-Dicarbonyl Compounds: Pyruvic Acid, Biacetyl and Glyoxal. J. Photochem. Photobiol., A 2001, 146 (1−2), 19− 27.
(20) Grosjean, D.; Williams, E. L.; Grosjean, E. Atmospheric Chemistry of Isoprene and of Its Carbonyl Products. Environ. Sci. Technol. 1993, 27 (5), 830−840.
(21) Andreae, M. O.; Talbot, R. W.; Li, S. M. Atmospheric Measurements of Pyruvic and Formic-Acid. J. Geophys. Res. 1987, 92 (D6), 6635−6641.
(22) Nguyen, T. B.; Bateman, A. P.; Bones, D. L.; Nizkorodov, S. A.; Laskin, J.; Laskin, A. High-Resolution Mass Spectrometry Analysis of Secondary Organic Aerosol Generated by Ozonolysis of Isoprene. Atmos. Environ. 2010, 44 (8), 1032−1042.
(23) Baboukas, E. D.; Kanakidou, M.; Mihalopoulos, N. Carboxylic Acids in Gas and Particulate Phase above the Atlantic Ocean. J. Geophys Res: Atmos 2000, 105 (D11), 14459−14471.
(24) Bao, L. F.; Matsumoto, M.; Kubota, T.; Sekiguchi, K.; Wang, Q. Y.; Sakamoto, K. Gas/Particle Partitioning of Low-Molecular-Weight Dicarboxylic Acids at a Suburban Site in Saitama, Japan. Atmos. Environ. 2012, 47, 546−553.
(25) Bardouki, H.; Liakakou, H.; Economou, C.; Sciare, J.; Smolik, J.; Zdimal, V.; Eleftheriadis, K.; Lazaridis, M.; Dye, C.; Mihalopoulos, N. Chemical Composition of Size-Resolved Atmospheric Aerosols in the Eastern Mediterranean During Summer and Winter. Atmos. Environ. 2003, 37 (2), 195−208.
(26) Chebbi, A.; Carlier, P. Carboxylic Acids in the Troposphere, Occurrence, Sources, and Sinks: A Review. Atmos. Environ. 1996, 30 (24), 4233−4249.
(27) Ho, K. F.; Lee, S. C.; Cao, J. J.; Kawamura, K.; Watanabe, T.; Cheng, Y.; Chow, J. C. Dicarboxylic Acids, Ketocarboxylic Acids and Dicarbonyls in the Urban Roadside Area of Hong Kong. Atmos. Environ. 2006, 40 (17), 3030−3040.
(28) Khwaja, H. A. Atmospheric Concentrations of Carboxylic-Acids and Related-Compounds at a Semiurban Site. Atmos. Environ. 1995, 29 (1), 127−139.
(29) Limbeck, A.; Puxbaum, H.; Otter, L.; Scholes, M. C. Semivolatile Behavior of Dicarboxylic Acids and Other Polar Organic Species at a Rural Background Site (Nylsvley, Rsa). Atmos. Environ. 2001, 35 (10), 1853−1862.
(30) Kawamura, K.; Kasukabe, H.; Barrie, L. A. Source and Reaction Pathways of Dicarboxylic Acids, Ketoacids and Dicarbonyls in Arctic Aerosols: One Year of Observations. Atmos. Environ. 1996, 30 (10−11), 1709−1722.
(31) Talbot, R. W.; Andreae, M. O.; Berresheim, H.; Jacob, D. J.; Beecher, K. M. Sources and Sinks of Formic, Acetic, and Pyruvic Acids over Central Amazonia 2. Wet Season. J. Geophys. Res. 1990, 95 (D10), 16799−16811.
(32) Kawamura, K.; Tachibana, E.; Okuzawa, K.; Aggarwal, S. G.; Kanaya, Y.; Wang, Z. F. High Abundances of Water-Soluble Dicarboxylic Acids, Ketocarboxylic Acids and Alpha-Dicarbonyls in the Mountaintop Aerosols over the North China Plain During Wheat Burning Season. Atmos. Chem. Phys. 2013, 13 (16), 8285−8302.
(33) Kawamura, K.; Yasui, O. Diurnal Changes in the Distribution of Dicarboxylic Acids, Ketocarboxylic Acids and Dicarbonyls in the Urban Tokyo Atmosphere. Atmos. Environ. 2005, 39 (10), 1945−1960.
(34) Kawamura, K.; Bikkina, S. A Review of Dicarboxylic Acids and Related Compounds in Atmospheric Aerosols: Molecular Distributions, Sources and Transformation. Atmos. Res. 2016, 170, 140−160.
(35) Veres, P. R.; Roberts, J. M.; Cochran, A. K.; Gilman, J. B.; Kuster, W. C.; Holloway, J. S.; Graus, M.; Flynn, J.; Lefer, B.; Warneke, C.; et al. Evidence of Rapid Production of Organic Acids in an Urban Air Mass. Geophys. Res. Lett. 2011, 38, L17807.
(36) Hall, G. E.; Muckerman, J. T.; Preses, J. M.; Weston, R. E.; Flynn, G. W. Time-Resolved FTIR Studies of the Photodissociation of Pyruvic-Acid at 193 nm. Chem. Phys. Lett. 1992, 193 (1−3), 77−83.
(37) Rincon, A. G.; Guzman, M. I.; Hoffmann, M. R.; Colussi, A. J. Optical Absorptivity Versus Molecular Composition of Model Organic Aerosol Matter. J. Phys. Chem. A 2009, 113 (39), 10512−10520.
(38) Closs, G. L.; Miller, R. J. Photoreduction and Photodecarboxylation of Pyruvic Acid. Applications of CIDNP to Mechanistic Photochemistry. J. Am. Chem. Soc. 1978, 100 (11), 3483−3494.
(39) Vesley, G. F.; Leermakers, P. A. Photochemistry of Alpha-Keto Acids + Alpha-Keto Esters 3. Photolysis of Pyruvic Acid in Vapor Phase. J. Phys. Chem. 1964, 68 (8), 2364−2366.
(40) Guzman, M. I.; Colussi, A. J.; Hoffmann, M. R. Photoinduced Oligomerization of Aqueous Pyruvic Acid. J. Phys. Chem. A 2006, 110 (10), 3619−3626.
(41) Dhanya, S.; Maity, D. K.; Upadhyaya, H. P.; Kumar, A.; Naik, P. D.; Saini, R. D. Dynamics of OH Formation in Photodissociation of Pyruvic Acid at 193 nm. J. Chem. Phys. 2003, 118 (22), 10093−10100.
(42) Griffith, E. C.; Carpenter, B. K.; Shoemaker, R. K.; Vaida, V. Photochemistry of Aqueous Pyruvic Acid. Proc. Natl. Acad. Sci. U. S. A. 2013, 110 (29), 11714−11719.
(43) Leermakers, P. A.; Vesley, G. F. Photolysis of Pyruvic Acid in Solution. J. Org. Chem. 1963, 28 (4), 1160−1164.
(44) O'Neill, J. A.; Kreutz, T. G.; Flynn, G. W. IR Diode-Laser Study of Vibrational-Energy Distribution in CO_2 Produced by UV Excimer Laser Photofragmentation of Pyruvic-Acid. J. Chem. Phys. 1987, 87 (8), 4598− 4605.
(45) Wood, C. F.; O'Neill, J. A.; Flynn, G. W. Infrared Diode-Laser Probes of Photofragmentation Products - Bending Excitation in CO_2 Produced by Excimer Laser Photolysis of Pyruvic-Acid. Chem. Phys. Lett. 1984, 109 (4), 317−323.
(46) Berges, M. G. M.; Warneck, P. Product Quantum Yields for the 350 nm Photodecomposition of Pyruvic-Acid in Air. Bur Bunsenges Chem. Phys. 1992, 96 (3), 413−416.
(47) Grosjean, D. Atmospheric Reactions of Pyruvic Acid. Atmos. Environ. 1983, 17 (11), 2379−2382.
(48) Yamamoto, S.; Back, R. A. The Photolysis and Thermal Decomposition of Pyruvic Acid in the Gas Phase. Can. J. Chem. 1985, 63 (2), 549−554.
(49) Davidson, R. S.; Goodwin, D.; Deviolet, P. F. The Mechanism of the Photoinduced Decarboxylation of Pyruvic-Acid in Solution. Chem. Phys. Lett. 1981, 78 (3), 471−474.
(50) Guzman, M. I.; Colussi, A. J.; Hoffmann, M. R. Photogeneration of Distant Radical Pairs in Aqueous Pyruvic Acid Glasses. J. Phys. Chem. A 2006, 110 (3), 931−935.
(51) Carlton, A. G.; Turpin, B. J.; Lim, H. J.; Altieri, K. E.; Seitzinger, S. Link between Isoprene and Secondary Organic Aerosol (SOA): Pyruvic Acid Oxidation Yields Low Volatility Organic Acids in Clouds. Geophys. Res. Lett. 2006, 33 (6), L06822.
(52) Stefan, M. I.; Bolton, J. R. Reinvestigation of the Acetone Degradation Mechanism in Dilute Aqueous Solution by the UV/H_2O_2 Process. Environ. Sci. Technol. 1999, 33 (6), 870−873.
(53) Saito, K.; Sasaki, G.; Okada, K.; Tanaka, S. Unimolecular Decomposition of Pyruvic Acid - an Experimental and Theoretical Study. J. Phys. Chem. 1994, 98 (14), 3756−3761.
(54) Taylor, R. The Mechanism of Thermal Eliminations XXIII: [1] the Thermal Decomposition of Pyruvic Acid. Int. J. Chem. Kinet. 1987, 19 (8), 709−713.
(55) Colberg, M. R.; Watkins, R. J.; Krogh, O. D. Vibrationally Excited Carbon-Dioxide Produced by Infrared Multiphoton Pyrolysis. J. Phys. Chem. 1984, 88 (13), 2817−2821.
(56) Plath, K. L.; Takahashi, K.; Skodje, R. T.; Vaida, V. Fundamental and Overtone Vibrational Spectra of Gas-Phase Pyruvic Acid. J. Phys. Chem. A 2009, 113 (26), 7294−7303.
(57) Larsen, M. C.; Vaida, V. Near Infrared Photochemistry of Pyruvic Acid in Aqueous Solution. J. Phys. Chem. A 2012, 116 (24), 5840−5846.
(58) Takahashi, K.; Plath, K. L.; Skodje, R. T.; Vaida, V. Dynamics of Vibrational Overtone Excited Pyruvic Acid in the Gas Phase: Line

Broadening through Hydrogen-Atom Chattering. J. Phys. Chem. A 2008, 112(32), 7321−7331.
(59) Chang, X. P.; Fang, Q.; Cui, G. L. Mechanistic Photodecarboxylation of Pyruvic Acid: Excited-State Proton Transfer and Three-State Intersection. J. Chem. Phys. 2014, 141 (15), 154311.
(60) da Silva, G. Decomposition of Pyruvic Acid on the Ground-State Potential Energy Surface. J. Phys. Chem. A 2016, 120 (2), 276−283.
(61) Kakkar, R.; Chadha, P.; Verma, D. A Theoretical Study of Structures and Unimolecular Decomposition Pathways of Pyruvic Acid. Internet Electron. J. Mol. Des. 2006, 5 (1), 27−48.
(62) Raczynska, E. D.; Duczmal, K.; Darowska, M. Keto-Enol Tautomerism in Pyruvic Acid - Theoretical (HF, MP2 and DFT in the Vacuo) Studies. Polym. J. Chem. 2005, 79 (4), 689−697.
(63) Murto, J.; Raaska, T.; Kunttu, H.; Rasanen, M. Conformers and Vibrational-Spectra of Pyruvic-Acid - an Ab Initio Study. J. Mol. Struct.: THEOCHEM 1989, 200, 93−101.
(64) Leermakers, P. A.; Vesley, G. F. Photochemistry of Alpha-Keto Acids and Alpha-Keto Esters 0.1. Photolysis of Pyruvic Acid and Benzoylformic Acid. J. Am. Chem. Soc. 1963, 85 (23), 3776−3779.
(65) Davidson, R. S.; Goodwin, D. The Role of Electron-Transfer Processes in the Photoinduced Decarboxylation Reaction of Alpha-Oxo-Carboxylic Acids. J. Chem. Soc., Perkin Trans. 2 1982, No. 12, 1559− 1564.
(66) Davidson, R. S.; Goodwin, D.; Pratt, J. E. The Mechanism of the Direct Photooxidative Decarboxylation of Alpha-Oxo-Carboxylic Esters. Tetrahedron 1983, 39 (7), 1069−1074.
(67) Rosenfeld, R. N.; Weiner, B. Energy Disposal in the Photofragmentation of Pyruvic-Acid in the Gas-Phase. J. Am. Chem. Soc. 1983, 105(11), 3485−3488.
(68) Schreiner, P. R.; Reisenauer, H. P.; Ley, D.; Gerbig, D.; Wu, C.-H.; Allen, W. D. Methylhydroxycarbene: Tunneling Control of a Chemical Reaction. Science 2011, 332 (6035), 1300−1303.
(69) Smith, B. J.; Nguyen, M. T.; Bouma, W. J.; Radom, L. Unimolecular Rearrangements Connecting Hydroxyethylidene (CH -
3 C-OH), Acetaldehyde (CH_3-CH O), and Vinyl Alcohol (CH_2 CH-OH). J. Am. Chem. Soc. 1991, 113 (17), 6452−6458.
(70) Winterhalter, R.; Jensen, N. R.; Magneron, I.; Wirtz, K.; Mellouki, A.; Mu, Y.; Tadic, Y.; Horowitz, A.; Moortgat, G.; Hjorth, J. Studies of the Photolysis of Pyruvic Acid: Products and Mechanism. In Proceedings of the EUROTRAC-2 Symposium 2000; Midgley, P. M., Reuther, M., Williams, M., Eds.; Springer: Berlin, 2001.
(71) Calvert, J.; Mellouki, A.; Orlando, J.; Pilling, M.; Wallington, T. Mechanisms of Atmospheric Oxidation of the Oxygenates; Oxford University Press: New York, 2011.
(72) Blitz, M. A.; Heard, D. E.; Pilling, M. J.; Arnold, S. R.; Chipperfield, M. P. Pressure and Temperature-Dependent Quantum Yields for the Photodissociation of Acetone between 279 and 327.5 nm. Geophys. Res. Lett. 2004, 31 (6), GL018793.
(73) Khamaganov, V. G.; Crowley, J. N. Pressure Dependent Photolysis Quantum Yields for $CH_3C(O)CH_3$ at 300 and 308 nm and at 298 and 228 K. Phys. Chem. Chem. Phys. 2013, 15 (25), 10500− 10509.
(74) Holmes, J. R.; O'Brien, R. J.; Crabtree, J. H.; Hecht, T. A.; Seinfeld, J. H. Measurement of Ultraviolet Radiation Intensity in Photochemical Smog Studies. Environ. Sci. Technol. 1973, 7 (6), 519−523.
(75) Szabo, E. Atmospheric Kinetics and Photochemistry of Oxygenated Volatile Organic Compounds. University of Lille 1 and University of Szeged: 2012.
(76) Atkinson, R.; Baulch, D. L.; Cox, R. A.; Crowley, J. N.; Hampson, R. F.; Hynes, R. G.; Jenkin, M. E.; Rossi, M. J.; Troe, J. Evaluated Kinetic and Photochemical Data for Atmospheric Chemistry: Volume I - Gas Phase Reactions of Ox, Hox, Nox and Sox Species. Atmos. Chem. Phys. 2004, 4 (4), 1461−1738.
(77) Rottman, G. J.; Woods, T. N. October, 1991, Updated Daily through March, 2004. The Upper Atmosphere Research Satellite (Uars) Solstice Solar Spectral Irradiance Dataset, Lisird (Lasp Interactive Solar Irradiance Data Center). http://lasp.colorado.edu/lisird/tss/uars_solstice_ssi.csv (accessed Nov. 12, 2015).
(78) Sander, S. P.; Abbatt, J.; Barker, J. R.; Burkholder, J. B.; Friedl, R. R.; Golden, D. M.; Huie, R. E.; Kolb, C. E.; Kurylo, M. J.; Moortgat, G. K., et al., Chemical Kinetics and Photochemical Data for Use in Atmospheric Studies, Evaluation Number 17; Jet Propulsion Laboratory: Pasadena, CA, 2011.
(79) Reva, I.; Nunes, C. M.; Biczysko, M.; Fausto, R. Conformational Switching in Pyruvic Acid Isolated in Ar and N2Matrixes: Spectroscopic Analysis, Anharmonic Simulation, and Tunneling. J. Phys. Chem. A 2015, 119 (11), 2614−2627.
(80) Gerbig, D.; Schreiner, P. R. Hydrogen-Tunneling in Biologically Relevant Small Molecules: The Rotamerizations of Alpha-Ketocarboxylic Acids. J. Phys. Chem. B 2015, 119 (3), 693−703.
(81) Arnett, J. F.; Larson, D. B.; Mcglynn, S. P. Absorption and Emission-Spectroscopy of Pyruvic Acids and Pyruvate Esters. J. Am. Chem. Soc. 1973, 95 (23), 7599−7603.
(82) Moortgat, G. K.; Meyrahn, H.; Warneck, P. Photolysis of Acetaldehyde in Air: CH_4, CO and CO_2 Quantum Yields. ChemPhysChem 2010, 11 (18), 3896−3908.
(83) Klan, P.; Wirz, J. Photochemistry of Organic Compounds: From Concepts to Practice; John Wiley and Sons: West Sussex, U.K., 2009.
(84) Steinfeld, J. I.; Francisco, J. S.; Hase, W. L. Chemical Kinetics and Dynamics, 2nd ed.; Prentice Hall: Upper Saddle River, NJ, 1998.
(85) Atkinson, R.; Baulch, D. L.; Cox, R. A.; Crowley, J. N.; Hampson, R. F.; Hynes, R. G.; Jenkin, M. E.; Rossi, M. J.; Troe, J. Evaluated Kinetic and Photochemical Data for Atmospheric Chemistry: Volume II - Gas Phase Reactions of Organic Species. Atmos. Chem. Phys. 2006, 6 (11), 3625−4055.
(86) Atkinson, R.; Baulch, D. L.; Cox, R. A.; Hampson, R. F.; Kerr, J. A.; Troe, J. Evaluated Kinetic and Photochemical Data for Atmospheric Chemistry - Supplement-Iii. Int. J. Chem. Kinet. 1989, 21 (2), 115−150.
(87) Horowitz, A.; Calvert, J. G. Wavelength Dependence of the Primary Processes in Acetaldehyde Photolysis. J. Phys. Chem. 1982, 86 (16), 3105−3114.
(88) Horowitz, A.; Kershner, C. J.; Calvert, J. G. Primary Processes in the Photolysis of Acetaldehyde at 3000 -a and 25-Degrees-C. J. Phys. Chem. 1982, 86 (16), 3094−3105.
(89) Leighton, P. A.; Blacet, F. E. The Photolysis of the Aliphatic Aldehydes II. Acetaldehyde. J. Am. Chem. Soc. 1933, 55, 1766−1774.
(90) Poisson, N.; Kanakidou, M.; Crutzen, P. J. Impact of Non-Methane Hydrocarbons on Tropospheric Chemistry and the Oxidizing Power of the Global Troposphere: 3-Dimensional Modelling Results. J. Atmos. Chem. 2000, 36 (2), 157−230.
(91) Paulot, F.; Wunch, D.; Crounse, J. D.; Toon, G. C.; Millet, D. B.; DeCarlo, P. F.; Vigouroux, C.; Deutscher, N. M.; Gonzalez Abad, G. G.; Notholt, J.; et al. Importance of Secondary Sources in the Atmospheric Budgets of Formic and Acetic Acids. Atmos. Chem. Phys. 2011, 11 (5), 1989−2013.
(92) Ito, A.; Sillman, S.; Penner, J. E. Effects of Additional Nonmethane Volatile Organic Compounds, Organic Nitrates, and Direct Emissions of Oxygenated Organic Species on Global Tropospheric Chemistry. J. Geophys. Res. 2007, 112 (D6), D06309. Ito, A.; Sillman, S.; Penner, J. E. Effects of Additional Nonmethane Volatile Organic Compounds, Organic Nitrates, and Direct Emissions of Oxygenated Organic Species on Global Tropospheric Chemistry. J. Geophys. Res. 2007, 112 (D6), D06309.
(93) Veres, P.; Roberts, J. M.; Burling, I. R.; Warneke, C.; de Gouw, J.; Yokelson, R. J. Measurements of Gas-Phase Inorganic and Organic Acids from Biomass Fires by Negative-Ion Proton-Transfer Chemical-Ionization Mass Spectrometry. J. Geophys. Res. 2010, 115, D23302.